Energy 107 (2016) 227–233

Contents lists available at ScienceDirect

Energy

journal homepage: www.elsevier.com/locate/energy

Performance analysis of a lunar based solar thermal power system with regolith thermal storage

Xiaochen Lu, Rong Ma, Chao Wang, Wei Yao*

Energy Conversion Research Center (ECRC), Qian Xuesen Laboratory of Space Technology, China Academy of Space Technology, P. O. Box: 5142-225, Beijing 100094, China

ARTICLE INFO

Article history:
Received 3 May 2015
Received in revised form
8 February 2016
Accepted 28 March 2016
Available online 27 April 2016

Keywords:
Solar thermal power system
Lunar regolith
Stirling generator
Finite-time thermodynamics

ABSTRACT

The manned deep-space exploration is a hot topic of the current space activities. The continuous supply of thermal and electrical energy for the scientific equipment and human beings is a crucial issue for the lunar outposts. Since the night lasts for periods of about 350 h at most locations on the lunar surface, massive energy storage is required for continuous energy supply during the lengthy lunar night and the in-situ resource utilization is demanded. A lunar based solar thermal power system with regolith thermal storage is presented in this paper. The performance analysis is carried out by the finite-time thermodynamics to take into account major irreversible losses. The influences of some key design parameters are analyzed for system optimization. The analytical results shows that the lunar based solar thermal power system with regolith thermal storage can meet the requirement of the continuous energy supply for lunar outposts.

1. Introduction

After US government proposed the ambitious manned Mars mission [1], the manned deep-space exploration becomes a hot topic of the current space activities [2,3]. Many nations have expressed interest in temporary outposts and permanent bases on the Moon and the Mars. These outposts would eventually require reliable and continuous power of 10s–100s kWe for many years [4]. The continuous supply of thermal and electrical energy for the scientific equipment and human beings is a crucial issue for the lunar outposts. Since the Moon night lasts for a period of about 350 h for most locations on the lunar surface, the significant launch mass is required for the energy storage if the traditional photovoltaic-battery power system is adopted. Even if the regenerative fuel cells [5] with high energy density of 500 Wh/kg are applied, the weight of the energy storage should be more than 6.7 tons. Another choice is the nuclear reactors which can deliver electric and thermal energy at a constant level during the lunar day and night [4,6]. However, the nuclear reactors do require additional mass for shielding radiation-sensitive payloads and measures to protect human beings from nuclear radiations during launch, operation and post-utilization.

ISRU (In-Situ Resource Utilization) can have a tremendous beneficial impact on robotic and human exploration of the Moon, Mars and other planets [7,8]. In the lunar outposts, it is very necessary to utilize in-situ resource effectively and sufficiently to minimize the hardware which must be brought from the Earth and reduce the mission cost significantly. Accordingly, the idea has been proposed to use lunar regolith for thermal energy storage and electrical power generation [9,10]. To improve the thermal conductivity and energy storage efficiency, some methods such as regolith–helium mixture [11], melting regime [12,13], and processed regolith [14–16] have been proposed, and the temperature evolution and distribution of the regolith energy storage system are analyzed [16], while detailed system performance is still needed.

Since Stirling engines have principal advantages of high efficiency and suitable for variable external heat sources, solar-powered Stirling engines are paid much attention in recent years on the Earth [17–20] and other planet [21] applications. Since solar energy is not available during two-thirds of the day on the Earth, some methods, such as solar/fuel hybrids [17], thermo-chemical energy storage [22], and phase-change energy storage [23] have been proposed.

A lunar based solar thermal power system with regolith thermal storage is presented and analyzed in this paper. In order to take into account important irreversible losses such as finite-rate heat transfer, regenerative heat losses, conductive thermal bridging

* Corresponding author. Tel.: +8610 68747483.
E-mail addresses: yaowei@qxslab.cn, yaowei@cast.cn (W. Yao).

http://dx.doi.org/10.1016/j.energy.2016.03.132
0360-5442/

Nomenclature

A	area, m^2
a	thermal diffusivity, m^2/s
C	concentrating ratio
C_p	specific heat at constant pressure, J/(kg·K)
C_v	specific heat capacity at constant volume per mole, J/(mol·K)
h	depth, m
k	thermal conductivity, W/(m·K)
k_0	heat leak coefficient, W/K
M	regenerative time constant, K/s
n	mole numbers of the working fluid, mol
P	power, W
Q	heat energy, J
$\dot{Q}$	heat transfer rate, W
$\dot{q}$	heat flux, W/m^2
R	ideal gas constant, J/(mol·K)
T	temperature, K
T_a	ambient temperature, K
T_c	temperature of the working fluid during isothermal heat rejection process, K
T_H	temperature of the heat source, K
T_h	temperature of the working fluid during isothermal heat absorption process, K
T_i	initial temperature, K
T_L	temperature of the heat sink, K
t	time, s
U	overall heat transfer coefficient, $W/(m^2 \cdot K)$
W	Work, J
z	coordinate in the vertical direction, m

Greek symbols

α	solar absorptivity
ε	infrared emissivity
ε_R	effectiveness of the regenerator
η_m	thermal efficiency at maximum power output
η_t	thermal efficiency
λ	ratio of volume during the regenerative processes
ρ	density, kg/m^3
σ	Stefan–Boltzmann constant, 5.67×10^{-8} $W/(m^2 \cdot K^4)$
τ	cyclic period, s

Subscripts and superscripts

max	maximum
R	regenerator
rad	radiator
rtr	regolith thermal reservoir
s	sun
sc	solar concentrator

losses and finite regeneration processes time, the finite-time thermodynamics [18,24–26] is applied to analyze the lunar based solar thermal power system.

2. System description and methodology

Fig. 1 presents the schematic of a lunar based solar thermal power system with regolith thermal storage. The system includes a solar concentrator, a regolith thermal reservoir, a high temperature fluid loop, a Stirling generator, a low temperature fluid loop, a thermal radiator with a radiation shield, etc. The processed regolith with thermal diffusivity which is several orders higher than that of the native regolith [11] is adopted in the regolith thermal storage.

Fig. 2 shows the working principle and the energy flow of the lunar based solar thermal power system. During the daytime, the solar energy is concentrated and reflected by the solar concentrator to the surface of the regolith thermal storage with high solar absorptivity. Accordingly, most of the solar radiation is absorbed and restored in the regolith thermal storage during the period of daytime, and a small part of the absorbed heat is dissipated to the environment by the surface thermal radiation. The restored thermal energy in the regolith thermal storage is transported to the hot end of the Stirling generator for power generation by the high temperature fluid loop during all the day–night cycle. The Stirling generator converts the thermal energy into mechanical energy and finally to electrical power. The waste heat is transported by the low temperature fluid loop from the cold end of the Stirling generator to the thermal radiator and finally dissipated to the space.

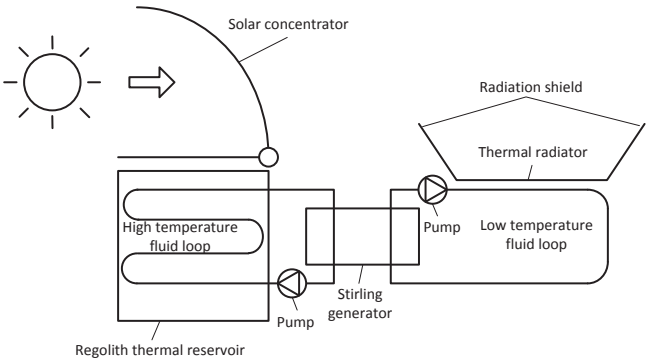

Fig. 1. Schematic of a lunar based solar thermal power system.

3. Theoretical model

3.1. Solar radiation

The solar radiation has significant difference at various places on the moon. For example, the equatorial solar flux on a unit horizontal surface varies sinusoidal during the daytime and vanishes during the lunar night with the peak heat flux about 1300 W/m^2. The time period of the solar flux is the synodic period, which is approximately 708 h [15]. While for the lunar north and south poles, the solar elevation angle would vary in a sinusoidal fashion from $-1.53°$ to $+1.53°$, and the longest lunar night is approximately 52 h [14]. For simplicity, the equatorial position with the longest lunar night is analyzed in this paper.

The solar heating of the regolith thermal storage can be enhanced by a concentrator that tracks the sun to direct the full solar flux to the regolith surface throughout the lunar day [16]. The solar flux on the surface of the regolith thermal storage becomes a square wave in this case, which can be written as,

$$\begin{aligned} \dot{q}_{sc}(t) &= C\dot{q}_{s,\max}, \quad nt_c \le t \le nt_c + t_d \\ \dot{q}_{sc}(t) &= 0, \quad nt_c + t_d \le t \le (n+1)t_c \end{aligned} \tag{1}$$

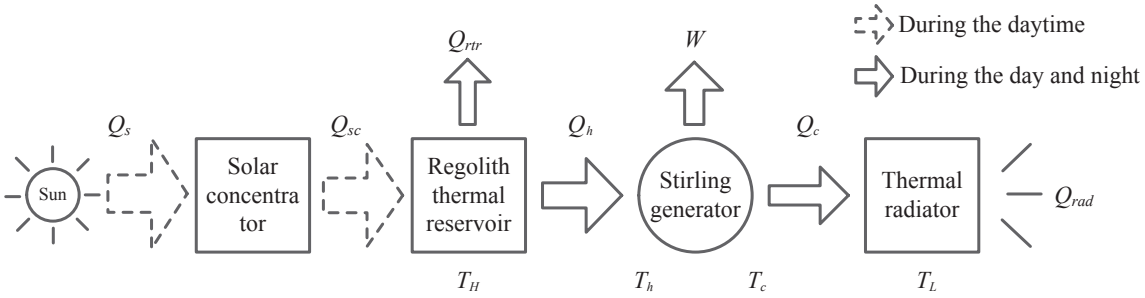

Fig. 2. Principle and energy flow of the lunar based solar thermal power system.

where n is the number of the day–night cycle, t_c and t_d are the periods of the day–night cycle and the daytime.

3.2. Regolith thermal reservoir

The processed regolith is adopted in the regolith thermal storage. Since the thermal conductivity of the processed regolith should be several orders higher than that of the native regolith, the side and bottom boundaries of the regolith thermal storage surrounded by the native regolith can be assumed to be adiabatic conditions. Previous research [15] showed that one dimensional model is sufficiently accurate for the regolith thermal reservoir. The equation governing the heat transfer in the regolith thermal reservoir can be written as,

$$\frac{\partial T}{\partial t} = a\frac{\partial^2 T}{\partial z^2}, \quad 0 \le z \le h \tag{2}$$

The boundary conditions are,

$$-k\left.\frac{\partial T}{\partial z}\right|_{z=0} = \alpha_{rtr}\dot{q}_{sc}(t) - \varepsilon_{rtr}\sigma\left(T^4 - T_a^4\right) \tag{3}$$

$$\left.\frac{\partial T}{\partial z}\right|_{z=h} = 0 \tag{4}$$

The solar absorptivity at the upper surface of the regolith thermal reservoir is assumed to be a constant and equal to 0.9. The emissivity of the upper surface of the regolith thermal reservoir is typically 0.9 during the day when the incident solar flux is nonzero, and is typically 0.25 during the nighttime when a radiation shield is used [15].

3.3. Stirling generator

An ideal Stirling cycle consists of four processes including two isothermal and two isochoric processes. In a real cycle, it is impractical to have a perfect heat exchange in the regenerator, in which the entire amount of absorbed heat is transferred to the working fluid during the next isochoric process, that is, a heat transfer loss (Q_R) may occur in the regenerator. In addition, a conductive heat transfer occurs between the hot end and cold end of the Stirling generator could result in a conductive thermal bridge loss (Q_0).

The heat losses during two regenerative processes per cycle is given by Refs. [24],

$$Q_R = nC_v(1-\varepsilon_R)(T_h - T_c) \tag{6}$$

where n is the mole number of the working fluid, C_v is the specific heat capacity of the working fluid per mole in the regenerative processes, ε_R is the effectiveness of the regenerator, T_h and T_c are temperatures of the working fluid in the high temperature isothermal process and in the low temperature isothermal process, respectively.

The conductive thermal bridging loss from the hot end at temperature T_H to the cold end at temperature T_L is assumed to be proportional to the cycle time and given by Refs. [26],

$$Q_0 = k_0(T_H - T_L)\tau \tag{5}$$

where k_0 is the heat leak coefficient between the hot and cold ends of the Stirling generator, and τ is the cyclic period.

The heat absorbed from the high temperature heat source and the heat released to the low temperature heat sink are,

$$Q_h = U_H A_H (T_H - T_h)t_1 = nRT_h \ln\lambda \tag{7}$$

$$Q_c = U_L A_L (T_c - T_L)t_2 = nRT_c \ln\lambda \tag{8}$$

where $\lambda = V_1/V_2$, is the ratio of volume during the regenerative processes, $U_H A_H$ and $U_L A_L$ are the products of the heat transfer coefficients and heat transfer area of the heat source and sink respectively.

Owing to the influence of irreversibility of the finite-rate heat transfer, the time of the regenerative processes is not negligible in comparison to that of the two isothermal processes [26]. In order to calculate the time of the regenerative processes, one assumes that the temperature of the working fluid in the regenerative processes as a function of time is given by:

$$t_3 = t_4 = (T_h - T_c)/M \tag{9}$$

where M is the proportionality constant which is independent of the temperature difference and dependent only on the property of the regenerative material, called regenerative time constant.

Accordingly, the cyclic period τ can be written as,

$$\begin{aligned}\tau &= t_1 + t_2 + t_3 + t_4 \\ &= \frac{nRT_h \ln\lambda}{U_H A_H (T_H - T_h)} + \frac{nRT_c \ln\lambda}{U_L A_L (T_c - T_L)} + \frac{2}{M}(T_h - T_c)\end{aligned} \tag{10}$$

Take into account the major irreversibility and the conductive thermal bridging losses mentioned above, the net heats absorbs from the heat source and dissipates to the heat sink are given as,

$$Q_H = Q_h + Q_0 + Q_R \tag{11}$$

$$Q_L = Q_c + Q_0 + Q_R \tag{12}$$

The power output and the thermal efficiency are given by,

$$P = \frac{W}{\tau} = \frac{Q_H - Q_C}{\tau} = \frac{T_h - T_c}{\frac{T_h}{U_H A_H (T_H - T_h)} + \frac{T_c}{U_L A_L (T_c - T_L)} + B_1 (T_h - T_c)} \quad (13)$$

$$\eta_t = \frac{Q_H - Q_C}{Q_H} = \frac{T_h - T_c}{T_h + A_1 (T_h - T_c) + [k_0 (T_h - T_c)][\tau]} \quad (14)$$

where $A_1 = C_v(1 - \varepsilon_R)/R \ln \lambda$, $B_1 = 2/nRM \ln \lambda$.

To maximize the power output, take the derivative of the Eq. (13) with respect to the temperature and equate it to zero, namely $\partial P/\partial T_h = 0$ and $\partial P/\partial T_c = 0$, the optimal working fluid temperature for this condition can be obtained.

$$T_h = \frac{T_H \sqrt{\frac{U_H A_H}{U_L A_L}} + \sqrt{T_H T_L}}{1 + \sqrt{\frac{U_H A_H}{U_L A_L}}} \quad (15)$$

$$T_c = \frac{T_L + \sqrt{T_H T_L \frac{U_H A_H}{U_L A_L}}}{1 + \sqrt{\frac{U_H A_H}{U_L A_L}}} \quad (16)$$

Therefore, the maximum power output and the corresponding optimal thermal efficiency of the Stirling generator are,

$$P_{\max} = \frac{K\left(\sqrt{T_H} - \sqrt{T_L}\right)^2}{1 + B_1 K\left(\sqrt{T_H} - \sqrt{T_L}\right)} \quad (17)$$

$$\eta_m = \frac{\eta_{CA}}{(1 + A_1 \eta_{CA}) + \frac{k_0 (T_H - T_L)\left(1 + B_1 K T_H \eta_{CA}^2\right)}{K T_H \eta_{CA}}} \quad (18)$$

where $K = U_H A_H U_L A_L / (\sqrt{U_H A_H} + \sqrt{U_L A_L})^2$, $\eta_{CA} = 1 - (T_L/T_H)^2$.

3.4. Thermal radiator

The waste heat from the Stirling generator is transferred to the low mass thermal radiator. The surface of the thermal radiation with high emissivity can reject the waste heat finally to the deep space by thermal radiation. The influence of the solar radiation and the infrared thermal radiation from the surrounding moon surface can be avoided by the additional radiation shield. The radiated heat flux can be estimated by,

$$\dot{Q}_{rad} = \varepsilon_{rad} A_{rad} \sigma \left(T_{rad}^4 - T_a^4\right) \quad (19)$$

Normally the radiator is facing the outer space with a background temperature only about 4 K, and the background radiation can be neglected in the calculation.

4. Results and discussion

In order to analyze the performance of the power generation system using processed lunar regolith as thermal energy storage materials, the default parameter values including the thermophysical properties of the processed lunar regolith and the parameters of the Stirling generator listed in Table 1 are used in our simulations.

The theoretical model in section 3 was coded and solved by MATLAB software and the simulation results of the system performance are presented in Figs. 3–4.

It is suggested that an in-situ lunar regolith with high solar absorptivity (0.9) and infrared emissivity (0.9), and a simple solar collector with concentrating ratio of 1 can be used in the lunar based solar thermal power system for the early stage manned exploration missions. The simulation results are presented in Fig. 3. It shows that after initializing from a uniform temperature of 100 K, the system can realize stable temperature oscillations after the second diurnal cycle. The maximum and minimum temperatures of the regolith thermal reservoir are about 386 K and 288 K respectively during stable temperature oscillations. From sunrise, the temperature of the regolith thermal reservoir increases rapidly for approximately 50 h, and then gradual increases until sunset. The temperatures of the working fluid at the hot end and the cold end of the Stirling generator, and the thermal radiator follow the same trends as the temperature variation of the regolith thermal reservoir. The temperature of the high temperature fluid is between 230 and 300 K. The liquid refrigerant with appropriate thermal properties, such as Freon, HCFC-123 for example, is proposed to be used as the working fluid for lunar applications. Fig. 3b shows the variations of the maximum power output and the corresponding optimal thermal efficiency of the solar thermal power system during diurnal cycles. It presents that the maximum power output is changed between 3172 W and 1808 W, which could provide continuous electric power to lunar outposts. When the system is working in a stable oscillations state, the corresponding optimal thermal efficiency is between 32.8% and 29.7%.

For the future large scale manned exploration missions, with the technology progress on high solar absorptivity, low infrared emissivity coating technology of the lunar regolith and the light-weight solar collector with higher concentrating ratio, the solar energy collection efficiency can be significantly improved. The lunar based solar thermal power system with solar absorptivity of 0.95, infrared emissivity of 0.1 and concentrating ratio of 10 is calculated and the simulation results are presented in Fig. 4. It shows that the system can also realize stable temperature oscillations after the second diurnal cycle. The maximum and minimum temperatures of the regolith thermal reservoir are about 1210 K and 532 K respectively during stable temperature oscillations. The temperature of the high temperature fluid is between 440 and 900 K. The liquid with appropriate thermal properties in the temperature range, such as liquid metal and molten salt, for example, liquid sodium and nitrate, is proposed to be used as the working fluid for lunar applications. As Fig. 4b shows, the maximum power output is changed between 11,619 W and 2764 W in the stable oscillations. The corresponding optimal thermal efficiency is mainly between 29.2% and 26.7%. Accordingly, with the high concentration ratio and the high solar absorptivity, low infrared emissivity coating, the maximum output power nearly increases 3 times and the solar energy collection efficiency can be significantly improved.

The influence of some key design parameters are analyzed for system optimization. The effects of the concentrating ratio C of the solar concentrator on the maximum power output and the corresponding optimal thermal efficiency of the system are shown in Fig. 5. It is observed that the maximum power output of the system increases significantly with larger concentration ratio C. The maximum power outputs of the system are 3172 W, 4294 W, 5071 W, and 5681 W when the corresponding values of the concentration ratio are 1, 2, 3, and 4 respectively. The corresponding optimal thermal efficiency increases with higher concentration ratio C. The corresponding optimal thermal efficiencies of the system are 32.8%, 34.0%, 34.5%, and 35.2% when the corresponding values of the concentration ratio are 1, 2, 3, and 4, respectively.

The effects of the thermal radiator area on the maximum power output and the corresponding optimal thermal efficiency of the system are shown in Fig. 6. It is seen from the figure that the maximum power output and the corresponding optimal thermal efficiency increase with the larger area of the thermal radiator. The maximum power outputs of the system are 2568 W, 3172 W,

Table 1
Default parametric values.

Parameter	Default value
The peak solar flux, q_{max}	1300 W/m^2
Thermal diffusivity of the processed lunar regolith, $a = k/(\rho \cdot c_p)$	8.7×10^{-7} m^2/s
Density of the processed lunar regolith, ρ	3000 kg/m^3
Specific heat of the processed lunar regolith, C_p	800 J/(kg·K)
Thermal conductivity of the processed lunar regolith, k	2.1 W/(m·K)
The absorptivity of the regolith thermal storage surface, α_{rtr}	0.9
The emissivity of the regolith thermal storage surface, ε_{rtr}	0.9(day),0.25(night)
The emissivity of the thermal radiator, ε_{rad}	0.9
The environment temperature, T_a	4 K
Overall heat transfer coefficient × area, $U_H A_H$, $U_L A_L$	200 W/K
Compression ratio of the working fluid, V_1/V_2	2
Heat leak coefficient, k_0	2.5 W/K
Effectiveness of the regenerator, ε_R	0.9
Concentrating ratio of the solar concentrator, C	1

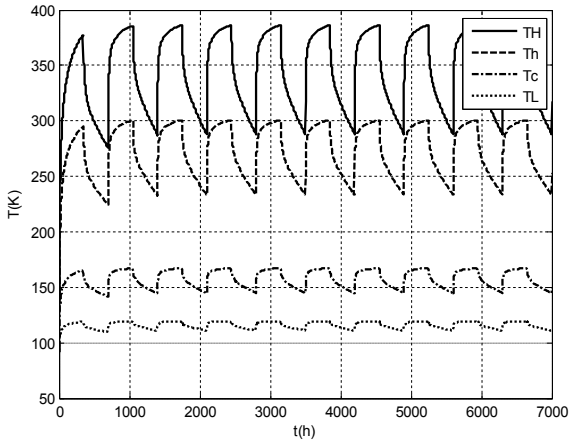

(a) Temperatures

T_H--temperature of the heat source, T_L--temperature of the heat sink

T_h--temperature of the working fluid during isothermal heat absorption process

T_c--temperature of the working fluid during isothermal heat rejection process

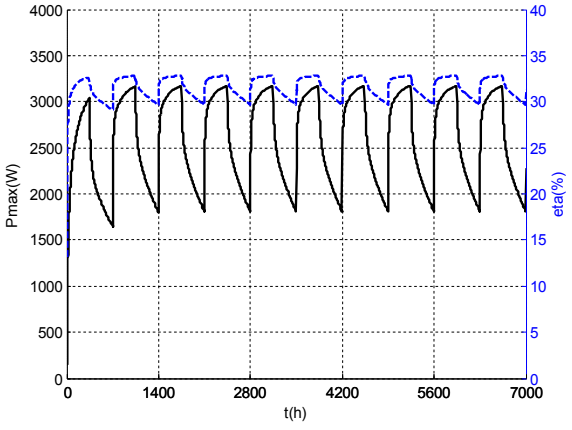

(b) Power and efficiency

Fig. 3. Simulation results of the solar thermal power system (C = 1, α_{rtr} = 0.9, ε_{rtr} = 0.9(day), 0.25(night)).

3532 W, 3788 W, and 3988 W when the corresponding values of the thermal radiator area are 500 m^2, 1000 m^2, 1500 m^2, 2000 m^2 and 2500 m^2 respectively. The corresponding optimal thermal efficiencies of the system are 30.1%, 32.8%, 34.3%, 35.2%, and 35.9% when the corresponding values of the thermal radiator area are 500 m^2, 1000 m^2, 1500 m^2, 2000 m^2 and 2500 m^2 respectively.

The effects of the heat leak coefficient on the maximum power output and the corresponding optimal thermal efficiency of the system are shown in Fig. 7. The maximum power outputs of the system are 3213 W, 3192 W, 3172 W, 3152 W, and 3132 W when the corresponding values of the heat leak coefficient are 0.5 W/K, 1.5 W/K, 2.5 W/K, 3.5 W/K and 4.5 W/K respectively. The corresponding optimal thermal efficiencies of the system are 37.7%, 35.1%, 32.8%, 30.8%, and 29.0% when the corresponding values of the heat leak coefficient are 0.5 W/K, 1.5 W/K, 2.5 W/K, 3.5 W/K and 4.5 W/K respectively. It is seen from the figure that the heat leak coefficient reduces the maximum power efficiency of the system. While, the maximum power output almost maintains unchangeable.

The effects of the effectiveness of the regenerator on the maximum power output and the corresponding optimal thermal efficiency of the system are shown in Fig. 8. The maximum power

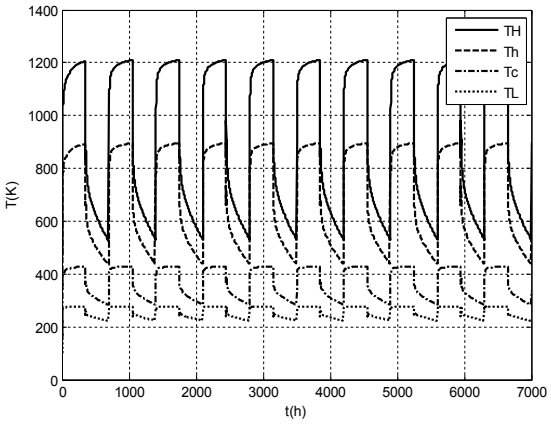

(a) Temperatures

T_H--temperature of the heat source, T_L--temperature of the heat sink

T_h--temperature of the working fluid during isothermal heat absorption process

T_c--temperature of the working fluid during isothermal heat rejection process

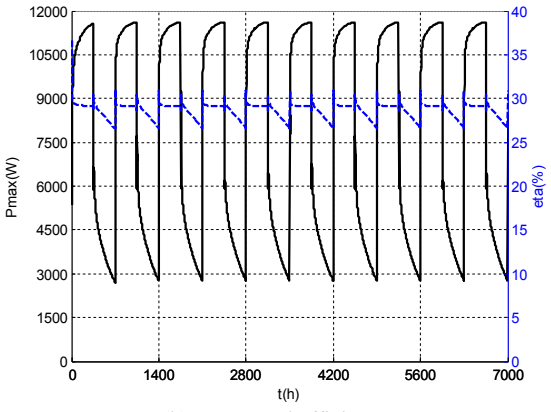

(b) Power and efficiency

Fig. 4. Simulation results of the solar thermal power system (C = 10, α_{rtr} = 0.95, ε_{rtr} = 0.1).

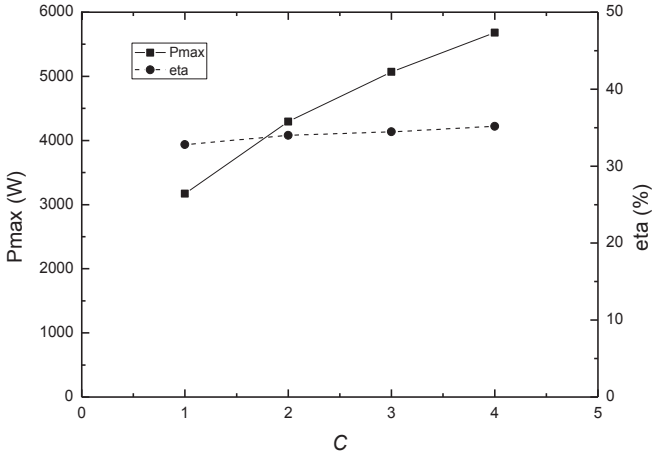

Fig. 5. Effect of the concentrating ratio *C*.

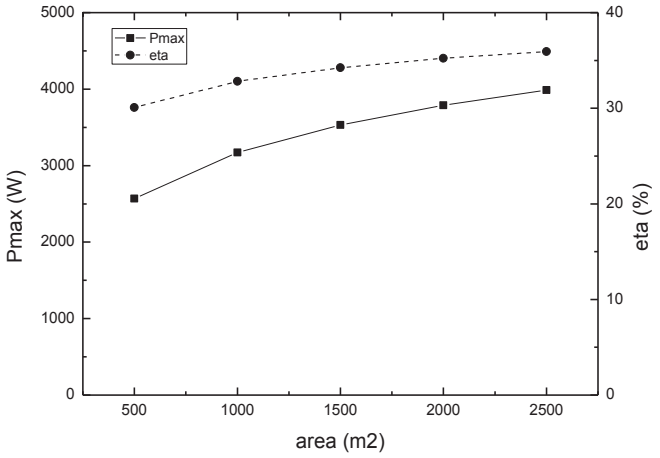

Fig. 6. Effect of the area of the thermal radiator.

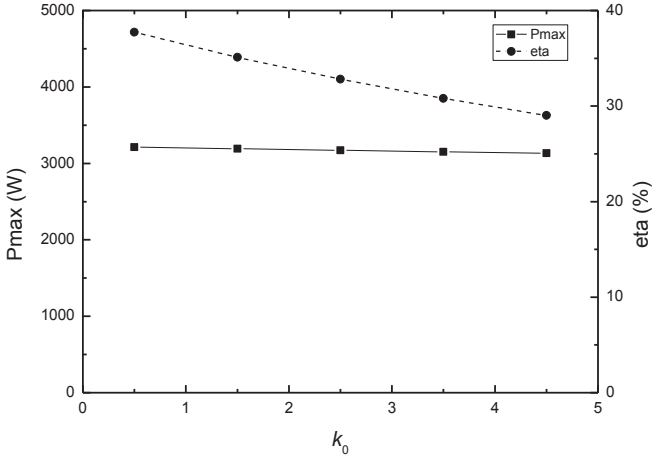

Fig. 7. Effect of the heat leak coefficient k_0.

outputs of the system are 2823 W, 2898 W, 2981 W, 3071 W, and 3172 W when the corresponding values of the effectiveness of the regenerator are 0.5, 0.6, 0.7, 0.8 and 0.9 respectively. The corresponding optimal thermal efficiencies of the system are 22.4%, 24.3%, 26.6%, 29.4%, and 32.8% when the corresponding values of

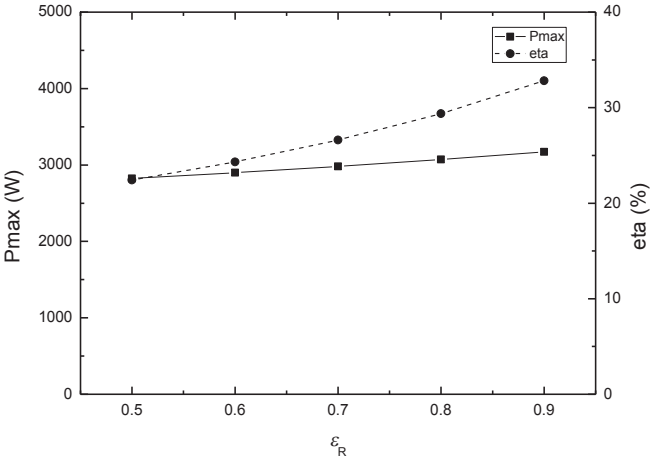

Fig. 8. Effect of the effectiveness of the regenerator ε_R.

the effectiveness of the regenerator are 0.5, 0.6, 0.7, 0.8 and 0.9 respectively. It is seen that the maximum power efficiency increases with the increment of the effectiveness of the regenerator. Therefore, the most efficient and cost effective regenerator should be used for the Stirling engine.

5. Conclusions

A lunar based solar thermal power system with regolith thermal storage is presented and the performance analysis is carried out by the finite-time thermodynamics to take into account major irreversible losses. The influence of some key design parameters are analyzed for system optimization. The main results are summarized as follows:

1) The lunar environment is suitable for the solar thermal power system with regolith thermal storage. The analysis shows that the temperature of the regolith thermal reservoir can be maintained high enough during lunar day–night cycles for power conversion. For an in-situ lunar regolith with high solar absorptivity (0.9) and infrared emissivity (0.9), and a simple solar collector with concentrating ratio of 1, the maximum and minimum temperatures of the regolith thermal reservoir are about 386 K and 288 K respectively during stable temperature oscillations. If a selective absorptive surface with high absorptivity (0.95) and low emissivity (0.1) and a high concentrating ratio (10) are used, the maximum and minimum temperatures of the regolith thermal reservoir increase to 1210 K and 532 K respectively during stable temperature oscillations.
2) The analytical results shows that the lunar based solar thermal power system with regolith thermal storage can meet the requirement of the continuous energy supply for lunar outposts. For an in-situ lunar regolith with high solar absorptivity (0.9) and infrared emissivity (0.9), and a simple solar collector with concentrating ratio of 1, when the system is working in a stable oscillations state, the power output is changed between 3172 W and 1808 W, and the corresponding optimal thermal efficiency is between 32.8% and 29.7%. If a selective absorptive surface with high absorptivity (0.95) and low emissivity (0.1) and a high concentrating ratio (10) are used, the power output is changed between 11,619 W and 2764 W, and the corresponding optimal thermal efficiency is mainly between 29.2% and 26.7%.
3) The influences of some key design parameters, such as the concentrating ratio, the area of the thermal radiator, the heat leak coefficient, and the effectiveness of the regenerator on the

maximum power output and the corresponding optimal thermal efficiency are analyzed. In order to achieve higher power output, it is desirable to increase the concentrating ratio and the area of the thermal radiator. In order to achieve higher efficiency, it is desirable to use a high efficiency regenerator and to have as small as possible heat leak coefficient.

Acknowledgment

The support of this work by the National Nature Science Foundation of China (Grants 51276191) is gratefully acknowledged.

References

[1] Bhattacharjee Y. Congress mostly approves new direction for NASA. Science 2010; 30 September. http://www.sciencemag.org/news/2010/09/congress-mostly-approves-new-direction-nasa.
[2] Viscio MA, Gargioli E, Hoffman JA, Maggiore P, Messidoro A, Viola N. A methodology for innovative technologies roadmaps assessment to support strategic decisions for future space exploration. Acta Astronaut 2014;94:813–33.
[3] Perino MA, Fenoglio F, Pelle S, Couzin P, Thaeter J, Eilingsfeld F, et al. Outlook of possible European contributions to future exploration scenarios and architectures. Acta Astronaut 2013;88:25–34.
[4] Schriener TM, El-Genk MS. Thermal-hydraulics and safety analyses of the solid core-sectored compact reactor (SC-SCoRe) and power system. Prog Nucl Energy 2014;76:216–31.
[5] Sone Y. A 100-W class regenerative fuel cell system for lunar and planetary missions. J Power Sources 2011;196:9076–80.
[6] El-Genk MS. Space nuclear reactor power system concepts with static and dynamic energy conversion. Energy Convers Manag 2008;49:402–11.
[7] Sanders GB, Larson WE. Progress made in lunar in-situ resource utilization under NASA's exploration technology and development program. J Aerosp Eng 2013;26(1):5–17.
[8] Anand M, Crawford IA, Balat-Pichelin M, Abanades S, van Westrenen W, Peraudeau G, et al. A brief review of chemical and mineralogical resources on the Moon and likely initial in situ resource utilization (ISRU) applications. Planet Space Sci 2012;74:42–8.
[9] Barna GJ, Johnsen RL. Investigation of the use of the lunar surface layer to store energy for generating power during the lunar night. 1968. NASA TM X-1560.
[10] Landis GA. Solar power for the lunar night. 1989. NASA TM 102127.
[11] Tillotson B. Regolith thermal energy storage for lunar nighttime power. 1991. NASA-CR-192881.
[12] Crane RA. Evaluation of in-situ thermal energy storage for lunar based solar dynamic systems. 1991. NASA-CR-189054.
[13] Colozza AJ. Analysis of lunar regolith thermal energy storage. 1991. NASA Contractor Report 189073.
[14] Wegeng RS, Humble PH, Sanders JH, Feier II, Pestak CJ. Thermal energy storage and power generation for the manned outpost using processed lunar regolith as thermal mass materials. In: AIAA SPACE 2009 conference & exposition; 14–17 Sptember 2009. Pasadena, California.
[15] Balasubramaniam R, Gokoglu S, Sacksteder K, Wegeng R, Suzuki N. Analysis of solar-heated thermal wadis to support extended-duration lunar exploration. J Thermophys Heat Transf 2011;25(1):130–9.
[16] Climent B, Torroba O, Gonzalez-Cinca R, Ramachandran N, Griffin MD. Heat storage and electricity generation in the Moon during the lunar night. Acta Astronaut 2014;93:352–8.
[17] Kongtragool B, Wongwises S. A review of solar-powered Stirling engines and low temperature differential Stirling engines. Renew Sustain Energy Rev 2003;7:131–54.
[18] Li Y, He Y, Wang W. Optimization of solar-powered Stirling heat engine with finite-time thermodynamics. Renew Energy 2011;36:421–7.
[19] Cheng CH, Yang HS, Keong L. Theoretical and experimental study of a 300-W beta-type Stirling engine. Energy 2013;59:590–9.
[20] Abdollahpour A, Ahmadi MH, Mohammadi AH. Thermodynamic model to study a solar collector for its application to Stirling engines. Energy Convers Manag 2014;79:666–73.
[21] Badescu V. Simulation of a solar Stirling engine operation under various weather conditions on Mars. J Sol Energy Eng 2004;126:812–8.
[22] Acharya S, Bhattacharjee S. Stirling engine based solar-thermal power plant with a thermo-chemical storage system. Energy Convers Manag 2014;86:901–15.
[23] Andraka CE. Dish Stirling advanced latent storage feasibility. Energy Procedia 2014;49:684–93.
[24] Kaushik SC, Kumar S. Finite time thermodynamic analysis of endoreversible Stirling heat engine with regenerative losses. Energy 2000;25:989–1003.
[25] Sahin AZ. Finite-time thermodynamic analysis of a solar driven heat engine. Exergy Int 2001;2:122–6.
[26] Kaushik SC, Kumar S. Finite time thermodynamic evaluation of irreversible ericsson and Stirling heat engines. Energy Convers Manage 2001;42:295–312.